APP Template V1.29 Article id: ejpaa09bd Typesetter: MPS Date received by MPS: 17/11/2015 PE: MAC003305 CE : LE:

IOP Publishing European Journal of Physics

Eur. J. Phys. **00** (2016) 000000 (12pp)

Design of an inexpensive integrating sphere student laboratory setup for the optical characterization of light sources

Frédéric B Leloup, Sven Leyre, Eva Bauwens, Toon Van den Abeele and Peter Hanselaer

Light & Lighting Laboratory, Department of Electrical Engineering (ESAT), KU Leuven, Gebroeders De Smetstraat 1, B-9000 Gent, Belgium

E-mail: Frederic.leloup@kuleuven.be

Received 24 August 2015, revised 30 October 2015
Accepted for publication 10 November 2015
Published DD MM 2016

Abstract

In this paper, the design of an inexpensive integrating sphere setup is presented, enabling students to perform optical characterization of light sources with reasonable accuracy, in a student laboratory context. Instead of using an expensive sphere with magnesium oxide or barium sulfate coating, a cheap polystyrene sphere is employed. In combination with a low-cost USB spectroradiometer, the system enables the direct measurement of the spectral radiant power of a light source. In addition to the radiant power, the luminous flux, luminous efficacy, and distinctive colorimetric quantities (colour coordinates, colour temperature, and colour rendering index) can be determined. Besides a description of the equipment used, the experimental measurement procedure and some typical measurement results are presented. A comparison between the data and the results obtained with scientific metrology instrumentation indicates reasonable accuracy. As a result, it can be concluded that the purpose of the presented experiments, being that students become acquainted with applications of radiometry and photometry, and with data collection and data analysis as in a professional context, is fully achieved with the described test setup.

Keywords: optical metrology, integrating sphere, radiometry, photometry

SQ1 (Some figures may appear in colour only in the online journal)

1. Introduction

The availability of reliable and accurate radiometric and photometric data is a basic requirement for the evaluation and comparison of the performance of light sources. Therefore,

standards and optical measurement methods providing specific guidelines and measuring conditions have been introduced, making it possible to compare different products on the same basis.

When measuring the radiant power or luminous flux, two basic methods are put forward: spatial resolved measurements using a goniometer, or spatial integrated measurements using an integrating sphere. Spatial resolved measurements include the determination of the luminous intensity distribution and suitable software integration (CIE 1996). This method requires a rather complicated measurement facility and is relatively time-consuming, but knowledge of the luminous intensity distribution pattern may be required for light planning purposes. Spatial integrated measurements involve considerably fewer readings and thus a faster determination of the luminous flux, obtained by comparison to the flux of a reference standard (CIE 1989, IES 2007). For both methods, the measurements can be performed photometrically using an illuminance meter as detector, or spectral radiometric data can also be recorded (Shaw and Goodman 2008, IES 2008).

Within the energy programme of the Master of Engineering Technology of KU Leuven, both measurement methods, as well as the related standards for determination of the luminous flux, are considered in courses on optics and lighting. While the theoretical part of these courses is lectured to the entire audience, an increased emphasis has been placed on individual supervision and evaluation of the students for the laboratory module. The laboratory module consists of three assignments, which the students have to perform over several weeks. Furthermore, students have to hand in a written assignment, in which they are asked to calculate and compare the luminous efficacy of two theoretical light sources, before and in preparation of the laboratory. In the end, a written test report has to be handed in, describing the results according to the guidelines as mentioned in the related standards. This way, students should be able to gain a deeper understanding of the specific topic areas of radiometry, photometry, and colorimetry. In order to admit several students simultaneously to the laboratory, multiple constructions of the same laboratory setup are required. Therefore, cheap alternatives to the expensive scientific metrology instrumentation, which still guarantee that the students get acquainted with optical metrology techniques and general radiometric and photometric quantities, are needed. This paper reports on the design of an inexpensive integrating sphere setup, enabling the optical characterization of light sources with reasonable accuracy in a student laboratory context.

2. Theoretical background

The integrating sphere is the most common and widely used device for determining optical characteristics of both materials and light sources (Yu *et al* 2006, Hanselaer *et al* 2009). The sphere is designed to achieve a homogeneous distribution of the optical radiation by means of multiple Lambertian reflections at the inner surface. When used to measure the radiant power and total luminous flux of a light source, the integrating sphere behaves as the input optical element for a detector of radiant power, placed at the exit port of the sphere. Depending on the type of emission of the light source (2π versus 4π steradian), the source can either be positioned in front of the sphere's entrance port or inside the sphere, respectively.

Consider a sphere with radius R. A certain spot (area dA_{src}) of the inner sphere wall emits specific radiation. Somewhere on the sphere wall, we locate a receiver (area dA_{rec}). The geometry of this situation is illustrated in figure 1. The basic definition for the illuminance detected by the receiver E_{rec} is given by

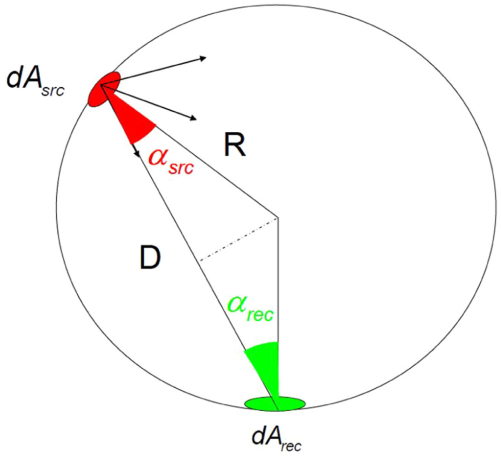

Figure 1. Geometry of the sphere with a source (src) and a receiver (rec).

$$E_{\text{rec}} = \frac{d\phi}{dA_{\text{rec}}}, \tag{1}$$

with $d\phi$ the infinitesimal incident flux on the infinitesimal receiver surface area dA_{rec}. Likewise, the luminance $L(\alpha_{\text{src}}, \beta_{\text{src}})$ from a source in a specific receiver direction can be defined as

$$L\left(\alpha_{\text{src}}, \beta_{\text{src}}\right) = \frac{d\phi^2}{dA_{\text{src}}.\ \cos\alpha_{\text{src}}.\ d\Omega_{\text{rec}}}. \tag{2}$$

α_{src} and β_{src} are the polar angles as seen from the source surface normal and azimuth angle, respectively. $dA_{\text{src}}.\ \cos\alpha_{\text{src}}$ represents the projected infinitesimal source surface as seen from the receiver position, $d\Omega_{\text{rec}}$ being the infinitesimal receiver solid angle. The latter can be written as

$$d\Omega_{\text{rec}} = \frac{dA_{\text{rec}}.\ \cos\alpha_{\text{rec}}}{D^2}, \tag{3}$$

in which α_{rec} and D are the polar angle as seen from the source surface normal and the distance between the source and the receiver, respectively. From these three basic definitions, the illuminance detected by the receiver E_{rec} can be rewritten as a function of the luminance $L(\alpha_{\text{src}}, \beta_{\text{src}})$

$$E_{\text{rec}} = L\left(\alpha_{\text{src}}, \beta_{\text{src}}\right).\ dA_{\text{src}}.\ \cos\alpha_{\text{src}}.\ \frac{\cos\alpha_{\text{rec}}}{D^2}. \tag{4}$$

This equation describes the contribution of each surface element dA_{src} to the receiver illuminance E_{rec}. The illuminance seems to be explicitly dependent on the locations of the source and the detector, due to the presence of the parameters $L(\alpha_{\text{src}}, \beta_{\text{src}})$, α_{src}, α_{rec}, and D in the equation. Yet, for a sphere the following relationships hold

$$\alpha_{\text{src}} = \alpha_{\text{rec}}, \tag{5}$$

$$D = 2.\ R.\ \cos\alpha_{\text{src}}. \tag{6}$$

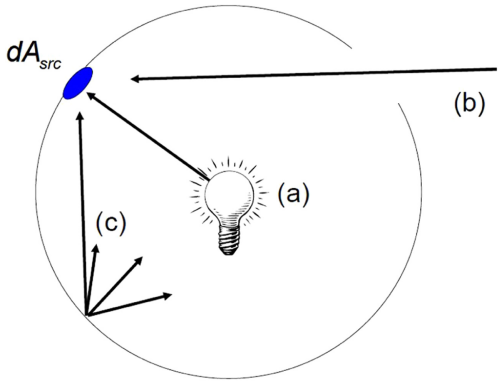

Figure 2. Schematic overview of the different contributions to the luminance $L(\alpha_{\text{src}}, \beta_{\text{src}})$ of a surface area dA_{src} within a sphere; (a) reflection of direct incident radiation of a light source, (b) reflection from direct incident radiation from outside the sphere, (c) reflection of light after multiple reflections on the sphere wall.

Therefore, (4) finally reduces to

$$E_{\text{rec}} = \frac{L(\alpha_{\text{src}}, \beta_{\text{src}}).\, dA_{\text{src}}}{4R^2}. \tag{7}$$

The illuminance becomes independent of the explicit positions of the source and the receiver anywhere on the sphere wall. Indeed, a smaller distance between source and receiver will be compensated for by the smaller projected surface areas. Yet, the sphere wall in itself is not the primary light source. The luminance of the sphere wall is caused by reflection of the radiation of a light source which is located in the sphere, or from reflection of an external beam incident through an open port, or from multiple reflections on other parts of the sphere wall (see figure 2). If the sphere wall is coated with a coating which is a Lambertian reflector, the luminance will not depend on the viewing direction anymore, and the receiver response will be totally independent of the location of the emitting and receiving surface. This characteristic offers the clue for measuring the total flux of a light source.

Under the ideal circumstances of a spherical geometry with infinitesimally small entrance and exit ports, and a sphere coating which behaves as a perfectly homogeneous Lambertian reflector with a total reflectance ρ being wavelength independent, the relation between the luminous flux of a light source ϕ_{src} and the receiver illuminance E_{rec} can be defined as

$$E_{\text{rec}} = \frac{1}{4\pi R^2}.\, \frac{\rho}{1-\rho}.\, \phi_{\text{src}} = f.\, \phi_{\text{src}}, \tag{8}$$

with f being defined as the sphere factor.

According to (8), the detector response should be the same if the same flux is introduced into the sphere, irrespective of the location of the direct impact on the sphere wall. This can be tested by using a narrow beam source, such as a laser diode. For each orientation of the beam, the same response should be recorded. The relative responsivity as a function of the location of the beam incident on the sphere wall is called the spatial response distribution function (SRDF) (Ohno 1998). In the ideal case, the SRDF should be constant.

Traditionally, specific coating materials such as barium sulfate (BaSO4) or magnesium oxide (MgO) are used for the sphere coating due to their high diffuse reflectance in the visible and near-infrared range of the spectrum (up to 99%), and due to their thermal stability until elevated temperatures of up to 350 °C, depending on the type of coating. Even using this type of material, in practice the ideal conditions cannot be met. For example, the reflectance value of the two sphere parts generally shows some degree of variability since they are coated separately (Knee 1999). Moreover, the surface of the detector itself can be considered as a deviation of the uniform diffuse coating requirement. Without any adaptations to the sphere geometry, the receiver also detects part of the light emitted by the source directly. This contribution is not taken into account in the calculation of (8), and is dependent on the luminance of the light source in the direction of the detector. As such, it will vary with the orientation of the source in the sphere (except for real isotropic sources). Therefore, the detector must be baffled against direct irradiation by the light source. However, this causes some important issues, since the field of view of the detector will no longer be the entire sphere surface due to the shielding effect of the baffle. As a consequence, the flux hitting the region of the sphere wall shadowed by the baffle or the face of the baffle oriented towards the light source will have to undergo at least one, respectively two, reflections before it can contribute to the detector signal. This results in a decrease of the SRDF in these regions, and a dependence of the detector response to the spatial distribution pattern of the light source (Ohno and Daubach 2001). Finally, the light source under test and its accessories also cause a source of measurement error (Miller and Ohno 2001, Liu *et al* 2008).

It must therefore be concluded that accurate absolute radiant power and total luminous flux measurements by use of an integrating sphere are not evident, since (8) is not valid in practice, and corrections are required (Hanselaer *et al* 2009). Yet, if the intensity distribution of two light sources is more or less identical, one can expect that the proportionality between the measured illuminance E_{rec} and the luminous flux ϕ_{src} still holds. As such, by application of the so-called 'substitution method' (CIE 1989), in which first a reference source with known luminous flux ϕ_{ref} is measured, followed by the light source under test, the luminous flux of the test source ϕ_{test} can be derived according to

$$\phi_{\mathrm{test}} = \phi_{\mathrm{ref}} . \frac{E_{\mathrm{test}}}{E_{\mathrm{ref}}}, \tag{9}$$

with E_{ref} and E_{test} representing the measured illuminance of the reference source and test source, respectively. In conclusion, since integrating sphere measurements suffer from low accuracy if spectral characteristics and angular intensity distributions of the test and reference source are dissimilar, test lamps should only be measured against standard lamps of the same or similar type.

3. Experimental setup

Instead of using an expensive research laboratory-based integrating sphere setup with a typical cost for the sphere alone of about €10 000 or more (detector not included), five measurement setups were constructed by use of cheap polystyrene spheres of diameter 50 cm. The diffuse and total reflectance of the sphere wall was measured with a HunterLab UltraScan PRO spectrophotometer. Both values correspond, indicating good scattering characteristics, and number about 82% over the visible wavelength range.

As an example, a picture of one setup is provided in figure 3, while a schematic overview of the entire measurement system is presented in figure 4. The lower part of the sphere is fixed

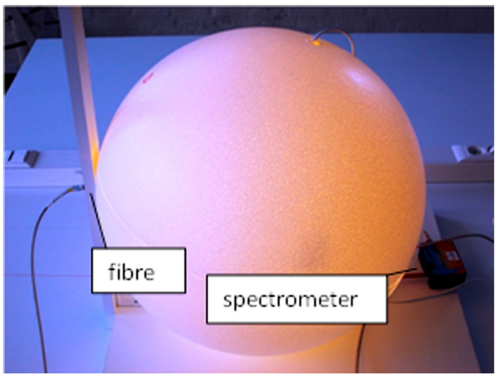

Figure 3. Picture of the polystyrene integrating sphere setup, including the optical fibre (Ocean Optics type QP200-2-VIS-BX) coupled to the USB-650 Red Tide spectrometer.

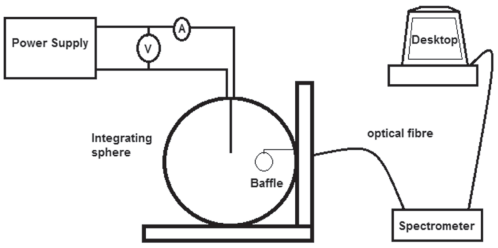

Figure 4. Schematic overview of the experimental integrating sphere setup.

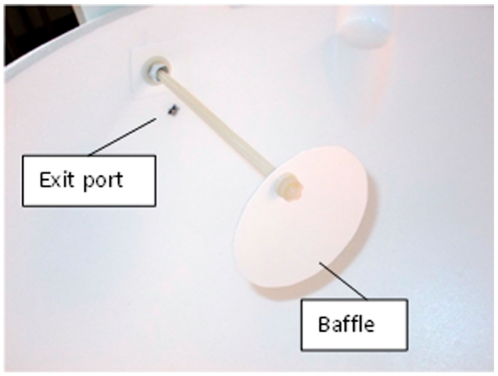

Figure 5. Inside the integrating sphere a baffle is mounted to prevent direct incident light from entering the optical fibre detector.

to a table holder, while the upper part of the sphere can be retrieved in order to insert the light source. A hole is drilled into the top of the upper half of the sphere, through which the wiring is allowed for driving the light source electrically by use of a power supply. A voltmeter and ammeter respectively record the voltage across and the current through the source under test.

A second whole is drilled into the side of the sphere in order to act as an exit port. A 2 m optical fibre with fibre core size of 200 μm (Ocean Optics type QP200-2-VIS-BX) is coupled

Table 1. Description of a typical set of test light sources.

Source type	Reference	Rated luminous flux (lm)	Rated power (W)
Tungsten halogen	Philips EcoClassic 28W E14 230V CL 2800K	370	28
Compact fluorescent lamp (CFL)	Philips Softone T45 5W 220-240V E14 WW 827	190	5
Light emitting fiode (LED)	16east LED Light Crystal LED Series Power Bulb B50 3100K	122	1.8

to this port via the table holder through an SMA 905 connector. A second SMA 905 connector connects the other end of the fibre to a spectrometer with incorporated charge coupled device (CCD) detector (Ocean Optics USB-650 Red Tide spectrometer, wavelength range 350–1000 nm). The preconfigured spectrometer is coupled to a desktop computer through a USB cable. Inside the sphere a baffle (diameter 8 cm) is mounted, preventing direct incident light from entering the detector (see figure 5). The price of the entire setup, including all the described parts and software (see further), is about €1500.

Eventually, a fibre splitter can be used to further lower the cost of the setup. A fibre splitter is composed of three fibres; two fibre legs on one side which overlap in a junction with a third fibre at the common end. This way, the signal acquisition of two sources, measured with two different integrating spheres, can be performed with just one spectrometer. Alternatively, the spectrometer detector can be replaced by an illuminance meter. However, this substitution will restrict the measurement results to only the photometric quantities of luminous flux and luminous efficacy.

For the processing of the measurement data, Logger Pro data-collection and analysis software is used. Alternatively, specific software tools for spectroscopy applications provided by the spectrometer manufacturer may be used (e.g. OceanView by Ocean Optics).

4. Measurement results

4.1. Determination of the spectral radiant power and total luminous flux of a set of light sources

The first assignment consists of the characterization of the optical and electrical performance of a set of light sources. Three types of light sources are selected; a description of a typical set of test sources is summarized in table 1.

To determine the radiant power and total luminous flux of the test sources, the substitution method as described in section 2 is put forward. As such, a reference light source has to be provided. In this case, an incandescent lamp (Gamma 40W 240 E14 Clear) with a theoretical total luminous flux of 390 lm is chosen for the purpose. The effective total luminous flux of the reference lamp together with the relative spectral distribution was measured in-house using a near-field goniophotometer, which in turn was calibrated with a reference lamp traceable to METAS, the Swiss Federal Institute of Metrology which provides internationally recognized calibration certificates (Audenaert *et al* 2015).

Since the intensity distribution of the reference light source and the test sources is more or less identical, i.e., they all have an omni-directional luminous intensity distribution, one can expect the proportionality between the measured illuminance and luminous flux (see (9)) to hold. At first, the power P_{ref} and the relative spectral radiant power $\phi_{e,\lambda,\mathrm{rel,ref}}$ of the

Table 2. Comparison of the rated total luminous flux of a typical set of test sources, as measured in the integrating sphere and near-field goniophotometer.

	Rated total luminous flux (lm)		
Source	Integrating sphere	Near-field goniophotometer	Rated power (W)
Tungsten halogen	308	317.4	29.6
CFL	205	238.3	5.24
LED	115	117.0	1.79

reference source with given total luminous flux ϕ_{ref} is measured. The integration time is thereby set to reach a CCD response just below saturation. A dark current correction is performed from a second measurement with the same integration time, but with the lamp turned off. For each pixel, the dark current corrected counts s^{-1} are linked to the incident spectral flux and used as a calibration file.

The entire procedure is repeated for the three test sources, taking into account the respective stabilization criteria of each type of lamp. This results in the knowledge of the spectral radiant power $\phi_{e,\lambda,\text{test}}$ of the test sources. Finally, the radiant power $\phi_{e,\text{test}}$ and total luminous flux ϕ_{test} of the test sources are calculated numerically, by taking into account the photopic eye sensitivity function V_λ. An overview of the results obtained for the three described test sources is provided in table 2.

By way of comparison, the total luminous flux and the power of each test source was also measured in the near-field goniophotometer. The results are also reported in table 2. As can be observed, the agreement between the results obtained with the two test instruments is satisfactory. Indeed, for the tungsten halogen and the light emitting diode (LED) test source, the relative difference numbers only 3% and 1.7%, respectively. For the compact fluorescent lamp (CFL) a larger deviation of almost 14% is observed. This larger deviation for CFL could be expected and arise from larger differences in the spectrum in comparison with the reference source spectrum, including the distinctive Hg emission lines as will be considered further below. Furthermore, it may be noticed that after a stabilization time of 2 h, the stabilization criteria of the CFL, as defined in the relevant approved method (IES 2011), were still not fulfilled. Instead of being below 1%, the per cent stability of six consecutive illuminance measurements taken 1 min apart was about 3%. Eventually, this might also have contributed to the larger differences found for the CFL.

4.2. Run-up time of a light source

Besides the characterization of the total luminous flux, a second assignment consists of the determination of the run-up time of a low-energy CFL. For this, the same measurement procedure as described in section 4.1. is employed, but measurements with the test source are recorded at given time intervals. After numerical integration of the measurement results, the total luminous flux can be visualized as a function of time.

The run-up time of a CFL is defined as the time required to reach a specified percentage (e.g. 80%) of the initial (stable) luminous flux, the time being measured from the moment the lamp circuit is energized (IEC 2001). As an example, the luminous flux of a CFL denoted as 'Carrefour 11W' is presented as a function of time in figure 6, with measurements performed every 15 s over a total period of 6 min. As can be noticed, the luminous flux increases rapidly

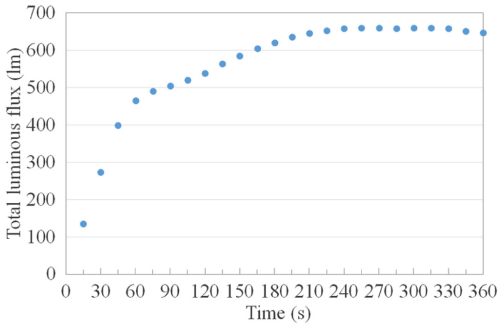

Figure 6. Graphical representation of the run-up time of a CFL denoted as Carrefour 11W.

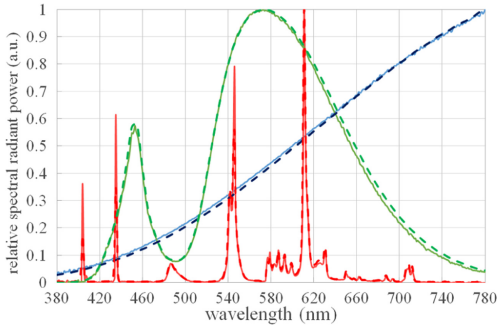

Figure 7. Graphical representation of the relative spectral radiant power $\phi_{e,\lambda,\mathrm{rel,test}}$ of three test light sources as a function of the wavelength λ, as measured with the integrating sphere setup (solid lines) and the near-field goniophotometer (dashed lines), respectively. Blue, green, and red curves correspond to the relative spectrum of the tungsten halogen source, LED, and CFL, respectively.

within the first 3 min, to moderately increase further before stabilizing to a value of about 650 lm after 6 min. According to figure 6, the run-up time of the example test source is calculated to be about 105 s (80% of the initial stable luminous flux).

4.3. Determination of colorimetric quantities of a set of light sources

Since the detector of the integrating sphere setup is composed of a spectrometer, not only the photometric but also the spectral properties of light sources may be determined. In the final colorimetry assignment, students are instructed to evaluate the colour coordinates, colour rendering index R_a and correlated colour temperature T_c of another set of light sources. These spectral characteristics are calculated numerically from the spectral radiant power $\phi_{e,\lambda,\mathrm{test}}$ of the sources, obtained following the procedure explained in section 4.1.

By way of example, the spectral characteristics of the three test sources described in table 1 were determined. In figure 7, the relative spectral radiant power $\phi_{e,\lambda,\mathrm{rel,test}}$ of the three sources, measured in the integrating sphere setup, is presented as a function of the wavelength λ (solid lines). By way of comparison, the relative spatially averaged spectra, as determined in the near-field goniophotometer according to the method using a spectroradiometer spatially scanned (IES 2008), are also depicted (dashed lines). A clear correspondence between the two

Table 3. Comparison between colorimetric quantities as calculated from measurements performed with the integrating sphere setup and with the near-field goniophotometer.

	Colour rendering index		Colour coordinates (x, y)		Correlated colour temperature (K)	
Source	Integrating sphere	Near-field goniophotometer	Integrating sphere	Near-field goniophotometer	Integrating sphere	Near-field goniophotometer
Tungsten halogen	100	100	(0.461;0.411)	(0.461;0.411)	2683	2687
CFL	76	80	(0.396;0.356)	(0.437;0.396)	3398	2930
LED	66	67	(0.430;0.423)	(0.424;0.416)	3271	3318

spectra for both the tungsten halogen source and the LED can be observed. For the CFL larger differences between the two spectra are observed, especially in the distinctive Hg emission lines around 404 nm, 435 nm, and 545 nm, where the relative spectral radiant power as measured in the integrating sphere is higher.

The resulting values of R_a, the colour coordinates (x, y), and T_c are collected in table 3. In line with the relative spectra, the calculated values from both methods correspond well for the tungsten halogen source as well as for the LED. For the CFL the value of T_c as calculated from the integrating sphere measurement is about 470 K higher than the value as calculated from the near-field goniophotometer measurement.

5. Conclusions

In this paper, the design of an inexpensive laboratory setup for the measurement of the total luminous flux of light sources has been presented. Instead of using an expensive laboratory-based sphere, a polystyrene sphere was used in combination with a low-cost USB spectro-radiometer. After having considered the theoretical approach of integrating sphere measurements, the experimental design of the alternative setup was discussed. The measurement procedure was explained by use of some real measurement examples. Further illustrative experiments were described, exemplifying the modularity and usefulness of the instrument. A comparison between the data and results obtained with scientific metrology instrumentation indicated a reasonable accuracy, with deviations ranging from a few to about 14%. As expected, the larger deviations were recorded for the CFL, for which the relative spectral radiant power around the distinctive Hg emission lines showed substantial differences.

The goal of the described experiments is to give students the opportunity to perform comprehensive illustrative optical experiments with reasonable accuracy as in a professional context. A significant emphasis is therefore also placed on the correct scientific representation of the results in a laboratory report, to be handed in after having performed the experiments. With the described test setup, which is about 7 to 10 times cheaper than the laboratory-based counterpart, these targets are absolutely fulfilled. Yet, further in-depth assignments may be formulated. For example, the uncertainty analysis of the measurement system might be considered. Therefore, the SRDF of the sphere may be characterized by use of a narrow beam source. This characterization will be considered in the near future.

Q1 ## References

Audenaert J, Acuna R P C, Hanselaer P and Leloup F B 2015 Practical limitations of near-field goniophotometer measurements imposed by a dynamic range mismatch *Opt. Express* **23** 2240–51

CIE1989 The measurement of luminous flux CIE Publication No. 84

CIE1996 The photometry and goniophotometry of luminaires CIE Publication No. 121

Hanselaer P, Keppens A, Forment S, Ryckaert W R and Deconinck G 2009 A new integrating sphere design for spectral radiant flux determination of light-emitting diodes *Meas. Sci. Technol.* **20** 095111

IEC2001 Self-ballasted lamps for general lighting services—performance requirements IEC Publication 60969

IES2007 Approved method for total luminous flux measurement of lamps using an integrating sphere photometer IES Publication LM-78-07

IES2008 Electrical and photometric measurements of solid-state lighting products IES Publication LM-79-08

IES2011 Electrical and photometric measurements of single-ended compact fluorescent lamps IES Publication LM-66-11

Knee P C 1999 Investigation of the uniformity and ageing of integrating spheres *Anal. Chim. Acta* **380** 391–9

Liu M-Q, Zhou X-L, Li W-Y, Chen Y-Y and Zhang W-L 2008 Study on methodology of LED's luminous flux measurement with integrating sphere *J. Phys. D: Appl. Phys.* **41** 144012

Miller C C and Ohno Y 2001 Luminous flux calibration of LEDs at NIST *Proc. 2nd CIE Expert Symp. on LED Measurement (CIE x022:2001)* pp 45–8

Ohno Y 1998 Detector-based luminous-flux calibration using the absolute integrating-sphere method *Metrologia* **35** 473–8

Ohno Y and Daubach R 2001 Integrating sphere simulation on spatial nonuniformity errors in luminous flux measurement *J. Illum. Eng. Soc.* **30** 105–15

Shaw M and Goodman T 2008 Array-based goniospectroradiometer for measurement of spectral radiant intensity and spectral total flux of light sources *Appl. Opt.* **47** 2637–47

Yu H L, Hsiao C C and Liu W C 2006 New apparatus for haze measurement for transparent media *Meas. Sci. Technol.* **17** N29–36

QUERY FORM

JOURNAL: European Journal of Physics

AUTHOR: F B Leloup *et al*

TITLE: Design of an inexpensive integrating sphere student laboratory setup for the optical characterization of light sources

ARTICLE ID: ejpaa09bd

The layout of this article has not yet been finalized. Therefore this proof may contain columns that are not fully balanced/matched or overlapping text in inline equations; these issues will be resolved once the final corrections have been incorporated.

SQ1
Please be aware that the colour figures in this article will only appear in colour in the online version. If you require colour in the printed journal and have not previously arranged it, please contact the Production Editor now.

Page 11

Q1
Please check the details for any journal references that do not have a link as they may contain some incorrect information.